AIP | Journal of Applied Physics

Enhanced photon-induced carrier density in silicon-on-insulator via surface recombination suppression for increasing plasma dispersion effect

Ming-Kai Hsieh, Kai-Ning Ku, and Ming-Chang M. Lee

Citation: J. Appl. Phys. **105**, 074510 (2009); doi: 10.1063/1.3106527

View online: http://dx.doi.org/10.1063/1.3106527

View Table of Contents: http://jap.aip.org/resource/1/JAPIAU/v105/i7

Published by the American Institute of Physics.

Enhanced photon-induced carrier density in silicon-on-insulator via surface recombination suppression for increasing plasma dispersion effect

Ming-Kai Hsieh,[1] Kai-Ning Ku,[1] and Ming-Chang M. Lee[1,2,a)]
[1]Institute of Photonics Technologies, National Tsing Hua Univeristy, Hsinchu, 30055 Taiwan, Republic of China
[2]Department of Electrical Engineering, National Tsing Hua Univeristy, Hsinchu, 30055 Taiwan, Republic of China

(Received 31 October 2008; accepted 22 February 2009; published online 9 April 2009)

The authors studied enhancement of photon-induced carrier density in silicon-on-insulator (SOI) by suppressing surface recombination. Through applying electric field at the top silicon surface or at the Si/SiO_2 interface, either electrons or holes are depleted near the interface, reducing the possibility of recombination. We examined enhanced photon-induced carrier density depending on the thickness of the SOI layer and the polarity of the applied field. The results show that the enhanced carrier density is prominent for thin SOI and increases with applied voltage. The effective photon-induced carrier density is magnified by three times with surface bias simultaneously at the top and bottom interfaces of SOI. The corresponding plasma dispersion effect is also estimated.
 [DOI: 10.1063/1.3106527]

I. INTRODUCTION

Silicon-on-insulator (SOI)-based optoelectronics progressed rapidly with state-of-the-art integrated-circuit (IC) technologies and received a lot of attention. Many sophisticated integrated photonics made by silicon waveguides were extensively reported[1–4] recently. However, due to the nature of indirect bandgap and lack of Pockel's effect in silicon, it is difficult to realize active functions for high-speed optical signal processing. One way to solve this issue is by taking advantage of the plasma dispersion effect through free-carrier injection.[5,6] The varied refractive index (Δn) induced by excess injected carrier density ($\Delta N_{e,h}$) is given by[7]

$$\Delta n = -(q^2\lambda^2/8\pi^2c^2\varepsilon_0 n)[\Delta N_e/m_e^* + \Delta N_h/m_h^*], \quad (1)$$

where q is the electronic charge, λ is the wavelength, c is the light speed, ε_0 is the permittivity of free space, n is the refractive index of c-Si, m_e^* is the effective mass of electrons, and m_h^* is the effective mass of holes. Photon-induced free-carrier injection is a potential in realizing all-optical modulation. Several applications such as high-speed signal modulation and switching have been demonstrated.[8–13] In general, achieving large dynamic range of refractive index variation usually requires high carrier injection typically more than 10^{17} cm^{-3} for lightly doped silicon photonic devices. Nevertheless, it is often challenging to attain such a high carrier density through common optical illumination because strong carrier recombination occurs near the surface of thin SOI, which is only submicron in thickness.

The dynamics of carrier density can be described by the continuity equation used for conventional semiconductor devices. The free-carrier density is generally controlled by the rates of electron-hole generation, recombination, and the divergence of current density as given by[14]

$$\begin{cases} \dfrac{\partial N_e}{\partial t} = G_e - R_e + \dfrac{1}{q}\nabla \cdot \mathbf{J}_e \\ \dfrac{\partial N_h}{\partial t} = G_h - R_h - \dfrac{1}{q}\nabla \cdot \mathbf{J}_h \end{cases}, \quad (2)$$

where $G_{e,h}$ is the carrier generation rate, $R_{e,h}$ is the carrier recombination rate, q is the electron charge, and $\mathbf{J}_e$ and $\mathbf{J}_h$ are the electron and hole current densities, respectively. The carrier generation rate depends on the intensity of external excitation, for example, optical illumination. The carrier recombination is governed by multiple processes including band-to-band recombination, Shockley–Read–Hall (SRH) recombination, surface recombination and Auger recombination. For p-type SOI with low-level injection, the recombination rate can be simply expressed by

$$R_e = \frac{\Delta N_e}{\tau_e} + \left(\frac{S_{top}}{d} + \frac{S_{bottom}}{d}\right)\Delta N_e, \quad (3)$$

where τ_e is the carrier lifetime in bulk silicon, d is the thickness of SOI, and S_{top} and S_{bottom} are the surface recombination velocities at the top and bottom interfaces of SOI, respectively. For bulk silicon, SRH recombination is the dominant process to annihilate electron-hole pairs. Nevertheless, for a thin SOI layer, surface recombination[15] can play an important role since there is a small thickness d. Surface-recombination-associated effective free carrier lifetime has been studied by microwave reflectance photoconductivity decay method.[16–18] In this article, we directly measured the static photoconductivity, which increased by applying electric field at the SOI interfaces. The corresponding photon-induced free carrier density was thus estimated from the measured conductivity. Other influential factors such as the SOI thickness and the polarity of the applied electric field were also examined. Via the increased carrier density, the plasma dispersion effect can be enhanced, aiding all-optical modulation for silicon photonics devices.

a)Electronic mail: mclee@ee.nthu.edu.tw.

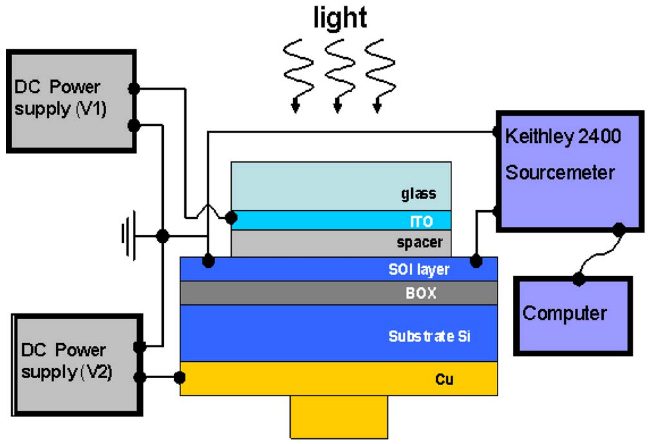

FIG. 1. (Color online) Experimental setup for measuring the photoconductivity of SOI with surface bias.

II. EXPERIMENTAL SETUP

The experimental setup is shown in Fig. 1. We used a halogen lamp (spectral range from 400 to 760 nm) as the light source with an intensity of 6.57 W/cm^2, measured by an integral sphere connected to a power meter. Such an incoherent light source has been demonstrated for creating image to simultaneously modulate multiple devices on a single chip through a commercial micromirror array.[19,20] To apply an electric field on the top SOI surface without blocking illumination in this experiment, a transparent indium tin oxide (ITO) glass was placed on the SOI and spaced by a thin polyethylene terephthalate film (100 μm thickness). We examined two SOI thicknesses: one is 340 nm and the other is 5 μm, which are conventional specifications for making silicon optical waveguides. Both the SOI layers are *p*-type with a resistivity of 14–22 Ω cm. The buried oxide (BOX) thickness is 1 μm and the substrate thickness is 500 μm. Two dc power supplies provided the top and bottom biases, respectively, and the Keithley 2400 sourcemeter was used for measuring the current-voltage (*I-V*) curve to extract the SOI conductance. These SOI layers were experimented as a metal-oxide-semiconductor field-effect transistor operated in the linear region. Nevertheless, the source and drain electrodes were prepared by casting silver epoxy on SOI without defining the heavily doped region and were separated by about 1 cm. In order to exclude the thermoresistivity effect, the whole setup was mounted on a copper base connected to a thermoelectric cooler for stabling the temperature. The substrate temperature was controlled at 30 °C.

III. MEASUREMENT RESULTS

We first inspected the photoconductivity without bias on SOI. The measured *I-V* characteristics between the source and drain before and after illumination for the 340 nm and the 5 μm SOI are shown in Fig. 2. The turn-on voltage is around 4 V due to Schottky contact on the electrodes. The photoconductances were derived by taking the linear slope of the *I-V* curves and were summarized in Table I. The values show that the thick SOI has large increase in conductance, which is about one order of magnitude greater than the thin SOI. Since the conductance is proportional to free-carrier density, we can conclude that the carrier density should increase accordingly under illumination although the concentration may not be uniform across the SOI layer. A possible reason for the increase in photon-induced carrier density for the thick SOI being larger is due to less surface recombination because of a relatively thick layer.

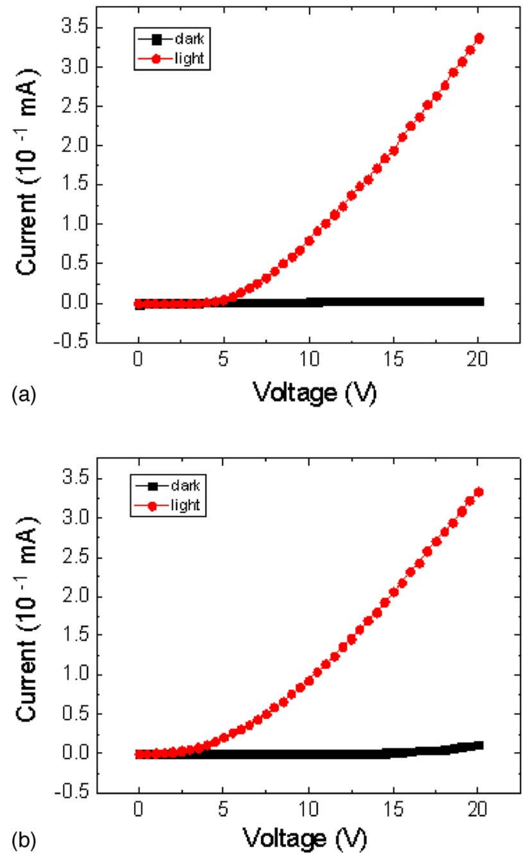

FIG. 2. (Color online) Measured *I-V* curves for (a) thick SOI (5 μm) and (b) thin SOI (340 nm) before and after illumination.

Since the surface recombination results from electron-hole pair annihilation through surface states within the bandgap, applying an electric field at the surfaces can deplete any of the two carriers, which reduces the possibility of recombination. To investigate the suppression of surface recombination, three bias conditions are studied: one is applying voltage on the top insulator layer above SOI, another is applying voltage on the bottom silicon substrate, and the other is applying voltages on the two sides simultaneously. Top bias prevents the recombination between the SOI and top cladding material and the bottom bias suppresses the recombination between the SOI and buried silicon dioxide.

TABLE I. Photon-induced conductance for the thick and the thin SOI. A slightly small dark conductance for the thick SOI is caused by variation in silicon resistivity and the size or distance between the tested electrodes.

	Dark conductance (A/V)	Light conductance (A/V)	Conductance enhancement ratio
Thin SOI (340 nm)	6.54×10^{-7}	2.15×10^{-5}	33
Thick SOI (5 um)	9.55×10^{-8}	2.27×10^{-5}	237

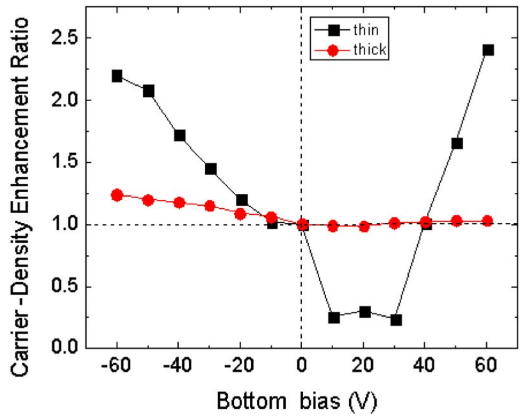

FIG. 3. (Color online) Photon-induced free-carrier density enhancement vs the bottom bias voltage for the thick and the thin SOI.

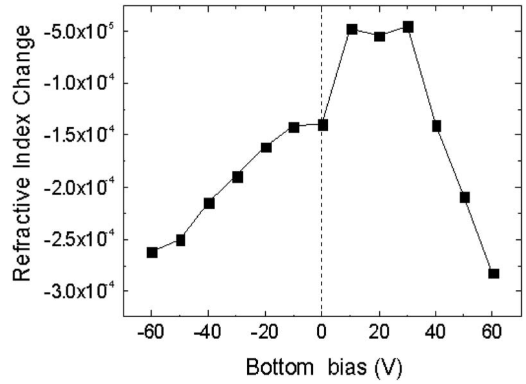

FIG. 4. The estimated effective refractive index change due to the photon-induced free carriers for the thin SOI vs the bottom bias voltage.

The bottom bias was first examined in this experiment. The silicon substrate was connected to a dc power supply while the SOI layer was electrically grounded under illumination. The voltage drop across the BOX varied from −60 to 60 V with an increase step of 10 V. For each increment, the *I-V* characteristics for the SOI layer were measured. Since the current increases as a linear function of applied voltage, the corresponding effective carrier density within the SOI layer can be estimated according to the observed photoconductance. Similar experiments were done for both the thin and the thick SOI samples, respectively. Normalized to the unbiased photon-induced carrier density, the electric-field-associated carrier enhancement ratios with respect to bias voltages are plotted in Fig. 3.

Since the measured photoconductance is much larger than the dark conductance, we can consider the induced free carriers primarily from optical illumination. In Fig. 3, the photon-induced carrier density generally increases with negative bias voltage. However, for positive bias voltage, the carrier density actually decreases first and then increases. Similar results are presented for both the thin and thick SOI. To give an insight into this phenomenon, we consider three interface conditions: accumulation, depletion, and inversion,[21] according to the metal-insulator-semiconductor model. In the case of accumulation or inversion condition, only one type of carriers (electrons or holes) is abundant near the interface while the other is almost extinct, which substantially inhibits the occurrence of surface recombination. On the other hand, as the interface is biased in the depletion condition, the commensurate highly injected photon-induced electrons and holes, which have much large density then the ionic impurity in the depletion region, can diffuse to the interface and recombine. According to experimental results, we can conclude that the accumulation occurs as the substrate is biased with negative voltage since the SOI is *p*-type and depletion and inversion take place with positive bias voltage. In addition, Fig. 3 shows that the carrier density enhancement for the thin SOI is much more significant than the thick SOI. It can be explained by the fact that surface recombination has a great impact on the static carrier density for the thin SOI. The corresponding effective refractive index change due to the photon-induced free carrier density versus the bottom bias voltage for the thin SOI is shown in Fig. 4.

Similarly, we did experiment to verify the influence from the top bias. Both the substrate and SOI layer were electrically grounded and the voltage was applied to the ITO glass. The bias voltage was varied from −900 to 900 V with an increment of 100 V. The measured carrier density enhancement under illumination is depicted in Fig. 5. The observed enhancement ratio is not as large as what we obtained via the bottom bias. The reason is due to the relatively thick spacer between the SOI and ITO glass, which has a thickness of 100 μm. However, like the bottom-bias experiment, the thin SOI exhibits a great change in the carrier density than the thick SOI. The corresponding refractive index variation due to the photon-induced free carriers with respect to the top bias is shown in Fig. 6.

If both the top SOI surface and the BOX interface are biased simultaneously, the surface recombination should be further suppressed. It was confirmed by testing several combinations of bias conditions and the result is listed in Table II. The thin SOI generally has a larger enhancement ratio than the thick SOI. Additionally, the enhancement ratio via the top and bottom biases simultaneously is larger than the single-surface bias, simply equivalent to two effects added together. The result agrees well with our prediction.

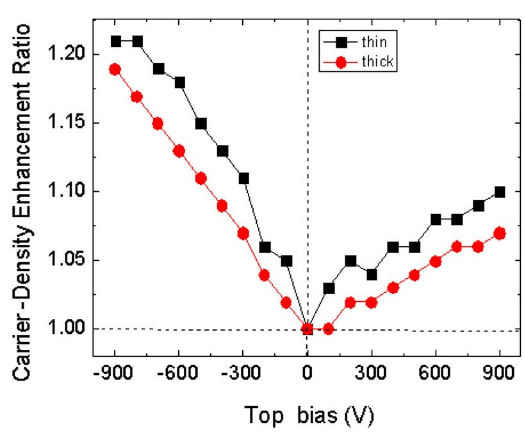

FIG. 5. (Color online) Photon-induced free-carrier density enhancement vs the top bias voltage for the thick SOI and the thin SOI.

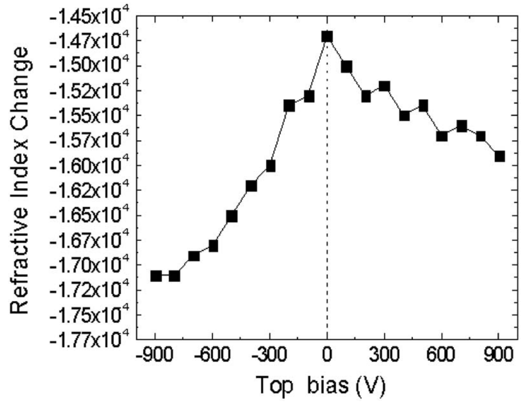

FIG. 6. The estimated effective refractive index change due to the photon-induced free carriers for the thin SOI vs the top bias voltage.

IV. CONCLUSION

We presented enhancement of photon-induced free-carrier density through surface bias on SOI. Via this bias, the surface recombination is suppressed to have higher carrier density under illumination. Thin SOI generally has a larger enhancement than thick SOI. The carrier density is also dependent on the polarity of bias voltage, which causes the interface in accumulation, depletion, or inversion condition. Two-side bias is better than single-side bias regarding carrier density enhancement, resulting from better surface recombination suppression. According to the experimental results, the photon-induced carrier density increases about three times with the two-side bias on a thin SOI. The corresponding plasma dispersion effect is also magnified. This study shows the potential using this surface bias for electro-optic or all-optical modulation in SOI-based photonic ICs.

TABLE II. Photon-induced free-carrier density enhancement ratio ($\Delta N/N_0$) under several bias conditions.

Top/bottom bias voltage [(V)/(V)]	Enhancement ratio (thin SOI)	Enhancement ratio (thick SOI)
+900/0	1.1	1.07
−900/0	1.21	1.19
0 60	2.41	1.03
0/−60	2.20	1.24
900/60	2.63	1.11
900/−60	2.38	1.38
−900/60	2.87	1.19
−900/−60	2.64	1.51

ACKNOWLEDGMENTS

This research work was funded by the National Science Council (Grant No. NSC-96-2628-E-007-143) and the National Nano-Device Laboratories (Grant No. NDL-P-96-2B-015) in Taiwan. The authors also thank Professor Yeh from the Institute of NanoEngineering and MicroSystem in the National Tsing Hua University for technical support.

[1] M. Lipson, J. Lightwave Technol. **23**, 4222 (2005).
[2] B. Jalali and S. Fathpour, J. Lightwave Technol. **24**, 4600 (2006).
[3] T. Baba, A. Sakai, T. Fukazawa, and F. Ohno, Trans. Inst. Electron. Commun. Eng. Jpn., Part C **88-C**, 363 (2005).
[4] R. A. Soref and J. P. Lorenzo, Solid State Technol. **31**, 95 (1988).
[5] S. Stepanov and S. Ruschin, Appl. Phys. Lett. **83**, 5151 (2003).
[6] S. Stepanov and S. Ruschin, Electron. Lett. **41**, 477 (2005).
[7] R. A. Soref and B. R. Bennett, IEEE J. Quantum Electron. **QE-23**, 123 (1987).
[8] O. Limon, A. Rudnitsky, Z. Zalevsky, M. Nathan, L. Businaro, D. Cojoc, and A. Gerardino, Opt. Express **15**, 9029 (2007).
[9] V. R. Almeida, C. A. Barrios, R. R. Panepucci, and M. Lipson, Nature (London) **431**, 1081 (2004).
[10] M. Belotti, J. F. Galisteo-Lopez, S. De Angelis, M. Galli, I. Maksymov, L. C. Andreani, D. Peyrade, and Y. Chen, Opt. Express **16**, 11624 (2008).
[11] B. G. Lee, A. Biberman, P. Dong, M. Lipson, and K. Bergman, IEEE Photon. Technol. Lett. **20**, 767 (2008).
[12] S. W. Leonard, H. M. van Driel, J. Schilling, and R. B. Wehrspohn, Phys. Rev. B **66**, 161102 (2002).
[13] M. Waldow, T. Plotzing, M. Gottheil, M. Forst, J. Bolten, T. Wahlbrink, and H. Kurz, Opt. Express **16**, 7693 (2008).
[14] S. M. Sze and K. K. Ng, *Physics of Semiconductor Devices*, 3rd ed. (Wiley-Interscience, New York, 2007).
[15] S. W. Glunz, A. B. Sproul, W. Warta, and W. Wettling, J. Appl. Phys. **75**, 1611 (1994).
[16] A. W. Stephens, A. G. Aberle, and M. A. Green, J. Appl. Phys. **76**, 363 (1994).
[17] T. Kuwayama, M. Ichimura, and E. Arai, Appl. Phys. Lett. **83**, 928 (2003).
[18] F. M. Schuurmans, A. Schonecker, A. R. Burgers, and W. C. Sinke, Appl. Phys. Lett. **71**, 1795 (1997).
[19] A. Jamshidi, P. J. Pauzauskie, P. J. Schuck, A. T. Ohta, P. Y. Chiou, J. Chou, P. D. Yang, and M. C. Wu, Nat. Photonics **2**, 85 (2008).
[20] P. Y. Chiou, A. T. Ohta, and M. C. Wu, Nature (London) **436**, 370 (2005).
[21] D. A. Neamen, *Semiconductor Physics and Devices*, 2nd ed. (IRWIN, New York, 1997).